SPE-196019-MS

Numerical Investigation to Understand the Mechanisms of CO_2 EOR in Unconventional Liquid Reservoirs

Fan Zhang, Imad A. Adel, I. W. R. Saputra, Weidong Chen, and David S. Schechter, Texas A&M University

This paper was prepared for presentation at the SPE Annual Technical Conference and Exhibition held in Calgary, Alberta, Canada, 30 Sep - 2 October 2019.

Abstract

Observations from pilot wells along with laboratory experiments have revealed the significant potential of CO_2 as an EOR agent in unconventional liquid reservoirs (ULR). This study focuses on unveiling the mechanisms of gas injection EOR through a combination of experimental results, ternary diagram analysis, and core-scale simulation. In addition, laboratory results were upscaled to the field-scale to evaluate the effectiveness of the CO_2 injection in production enhancement from ULR.

Gas injection experiments were performed at different pressures, and the laboratory results were upscaled to evaluate the production enhancement through gas injection EOR in ULR. A CT-generated core-scale model was utilized to investigate the mechanisms of gas injection EOR. Mechanisms such as diffusion and multi-contact miscibility were determined from core-scale simulation through history-matching experimental results, then upscaled to the field-scale model. Ternary diagrams reveal that EOR by gas injection is only effective at pressures greater than the Minimum Miscibility Pressure (MMP). Alteration of the injected gas and composition of crude oil clearly has an implication on changing the ternary diagram.

The primary production mechanisms of CO_2 EOR are multi-contact miscibility, vaporizing/condensing gas drive, oil swelling, and diffusion. Gas injection experiments recovered up to 45% of the Original Oil In Place (OOIP) at 3,500 psi, but the recovery factor was less than 5% when operating below the MMP. Diffusion has a minor effect in enhancing oil recovery in ULR based on the core-scale history-matching results. The multi-contact miscibility is found to be the primary driving mechanism for oil extraction during gas injection. Ternary diagrams analysis clearly demonstrates that MMP plays a significant role in gas injection and that miscible conditions need to be achieved for EOR projects in ULR. CT-scan technology is utilized to demonstrate the movement of the fluids inside the cores throughout the experiments. Thus, we can determine the high flow path regions of the core plugs. Additionally, the impact of injection pressure and the start time of the gas injection process were analyzed using the field-scale model. The simulation results indicate that gas injection has significant potential of enhancing oil production in ULR. This study not only reveals the mechanisms of gas injection in ULR, but also provides a method for designing and optimizing gas injection for Huff-n-Puff EOR.

This study challenges the paradigm that diffusion is the dominating parameter of CO_2 injection EOR in ULR. The novelty comes from the establishment of gas injection EOR mechanism in ULR through

a thorough analysis of laboratory experiments, core-scale simulation, and ternary diagram analysis. In addition, a new modeling workflow for the design of gas injection strategies is proposed to unveil the real potential of gas injection.

Introduction

The oil production from unconventional shale reservoirs has shown a significant increase since the last decade due to the implementation of horizontal drilling and multi-stage hydraulic fracturing (Xue et al. 2018; Yang et al. 2018; Zhang and Zhu 2017; Zhu et al. 2018). The interaction between hydraulic fractures and natural fractures create flow path networks, which provide a sufficiently high flow zone for oil production from unconventional shale reservoirs (Adel et al. 2016; Kou et al. 2018; Tang et al. 2017; Tang et al. 2018; Yang et al. 2017). Although there is already a significant volume of hydrocarbons being produced from shale reservoirs, the recovery factors for shale reservoirs are typically deficient (less than 10%). Therefore, it is essential to understand the transport mechanisms between fractures and matrix, in order to apply enhance oil recovery (EOR) techniques to improve oil recovery and extend the life of the wells in ULR (Bao and Gildin 2017; Bao et al. 2017; Deng and King 2015, 2018; Pan et al. 2019; Tang et al. 2018; Yang et al. 2016; Zhang and Zhu 2019).

Gas injection EOR and Surfactant-Assisted Spontaneous Imbibition (SASI) EOR techniques have presented a significant potential to enhance oil production in unconventional liquid reservoirs (Afra et al. 2019a). Field observations, along with laboratory data, reveal that both gas injection and SASI EOR result in additional oil recovery from shale reservoirs. Several researchers investigated the potential of SASI as an EOR technique in ULR through laboratory experiments (Alhashim et al. 2019; Alvarez et al. 2018; Alvarez and Schechter 2017; Saputra and Schechter 2018; Zhang et al. 2018b, 2019a; Zhang et al. 2018c; Zhang et al. 2019b). The primary mechanisms of SASI EOR are wettability alteration and interfacial tension (IFT) reduction caused by the interaction of the surfactant with the oil/water/rock system. In addition, there are some publications regarding the effectiveness of surfactant in stimulation fluid and upscaling laboratory results to the field scale through analytical methods and numerical simulation (Afra et al. 2018; Afra et al. 2019b). Simulation and upscaling results are consistent with laboratory observations that the addition of surfactant leads to higher oil recovery in ULR. Gas injection EOR technique has also been studied through laboratory experiments and numerical simulation. Several researchers are investigating the potential of gas injection EOR through Huff-n-Puff experiments. CO_2 presents a significant potential as an EOR agent to enhance oil recovery from shale core plugs. Also, there are several publications that studied the effectiveness of cyclic gas injection through numerical simulation using different gases, such as CO_2 and natural gas. Simulation results agreed with laboratory observation that gas injection enhances oil production in shale reservoir.

In earlier publications (Adel et al. 2018a; Adel et al. 2018b; Tovar et al. 2018a, b; Zhang et al. 2018a), we presented an overall evaluation of CO_2 injection as an EOR technique in ULR. CO_2 Huff-n-Puff experiments were performed on both preserved and re-saturated side-wall core plugs. The experimental results using preserved core plugs revealed the potential of CO_2 to extract oil from shale plugs, but lack of data of the initial oil in place (OOIP) in the preserved core plugs lead made it impossible to quantify the recovery factors. Therefore, we developed a workflow to clean and re-saturated the core plugs, allowing us to determine the oil in place OOIP and accurately determine the recovery factors.

Our results revealed that the recovery factor has a positive trend with pressure and soak time. Pressure plays a more significant role than soak time; higher injection pressures result in higher oil recoveries. We also analyzed the effect of the minimum miscibility pressure (MMP) on recovery factors and discovered that establishing miscibility is not enough as is the case in conventional reservoirs. The recovery factor from gas injection experiments is less than 5% when the injection pressure is below the MMP. However, the recovery factor keeps increasing with pressure beyond the MMP. The mechanism of gas injection EOR in the unconventional reservoirs is different than in conventional reservoirs, resulting in a main departure from the conventional paradigm that pressure at MMP is sufficient to achieve maximum oil recovery during the gas injection process.

The mechanisms of gas injection EOR in ULR include multi-contact miscibility, diffusion, vaporization drive gas, and oil swelling. During the soak period in the gas injection process, miscibility is established through the multi-contact process when the injection pressure is above the MMP. Lighter and intermediate components of oil are vaporized into the gas phase, resulting in additional oil production from the shale matrix. Based on Fick's law, the diffusion process occurs when a concentration difference exists. There is a significant concentration difference between the gas phase and the oil phase, which leads to oil and gas exchange on the interface. Both mechanisms cause extra oil production from the matrix and consequently result in oil production enhancement in ULR.

To understand the primary mechanisms of gas injection EOR, we study and integrate a combination of laboratory experiments, ternary diagram, and numerical simulation. Ternary diagrams and pseudo-ternary diagrams have been used for decades to visualize the phase behavior of gas-oil systems, such as a Methane-n-Butane-Decane system could be plotted in a ternary diagram (Reamer, 1949). Compositions of co-existing phases in the system were determined experimentally in stainless steel chambers at a given pressure and temperature. We used a ternary diagram to represent the vaporization gas drive process and to analyze the effect of pressure on improving the recovery factors in shale reservoirs. Ternary diagrams play a significant role in the numerical analysis of the gas injection process.

Due to the high cost of a gas injection pilot well, we use numerical simulation as a feasible approach to investigate the performance of gas injection EOR in the field scale. Several investigations of gas injection EOR in shale reservoirs were conducted through numerical simulation using different gases (Hoffman 2012; Kumar et al. 2015; Sun et al. 2016; Wan et al. 2013; Zou and Schechter 2017). These investigations demonstrate that gas injection EOR is a technically feasible method of recovering additional oil from unconventional liquid reservoirs. However, most of them did not incorporate laboratory experiments and data, and the mechanism of the simulation models is limited to pressure maintenance. Some researchers claim that the primary mechanism of gas injection EOR is diffusion because the diffusion coefficient is the only parameter that can be used to tune the model to represent the effect of gas injection. Although there is some limitations to numerical simulation, a robust model considering laboratory experiments, CT scan technology, and validated by history matching can provide a reasonable estimation of oil production enhancement from gas injection in ULR.

In this study, we investigate the mechanisms of CO_2 EOR through experimental laboratory results, ternary diagram, and numerical simulation. A comprehensive and systematic CO_2 EOR simulation workflow is developed to understand the mechanisms and to test the effect of oil production enhancement from gas injection in ULR. The core-scale simulation model is constructed using CT-scan technology which then is used to execute history matching on the laboratory data. Diffusion coefficient achieved from the core-scale simulation is then implemented into the field-scale model. The field-scale model incorporates hydraulic fracturing simulation and validated by history matching of an actual producing well. We investigate the efficiency and economics of CO_2 EOR on the field-scale model and evaluate the effect of operating pressures, injection volumes, soak times, and the start time of CO_2 EOR.

Methodology

The mechanisms of CO_2 EOR are multi-contact miscibility, diffusion, gas vaporization drive, and oil swelling. In order to reveal the primary mechanisms of CO_2 EOR, we consider experimental results of gas injection test, ternary diagram analysis, and numerical simulation. Experimental observations not only prove the potential of CO_2 as an EOR agent in unconventional reservoirs, but also provide an insight on the mechanisms of CO_2 EOR. Ternary diagram analysis explains the impact of pressure on improving oil recovery and validates that multi-contact miscibility is a main drive for CO_2 EOR. Core-scale history match simulation provides evidence that multi-contact miscibility is the primary mechanism.

A robust workflow of the simulation model was developed incorporating hydraulic fracturing simulation results, laboratory experiments, and history matching results. The validated field-scale is utilized to investigate the effectiveness of CO2 EOR in unconventional liquid reservoir. Evaluation of injection pressures, injection volumes, soak times, and the start time of CO_2 EOR application provides evidence for CO_2 EOR design.

CO_2 Injection Experimental Procedure

All the gas injection experiments were performed at reservoir temperature, which is 170 °F for the Eagle Ford formation. We developed a physical representation of hydraulic fractures by surrounding the shale core plug with glass beads. This setup is assembled into an aluminum core-holder which is scanned in a CT scanner. Fig. 1 demonstrates the schematic of the core-holder, which is utilized in all gas injection experiments. After the rock-fracture system is packed into the core-holder, we perform the huff-n-puff experiments for all Eagle Ford core plugs at different pressure. CO_2 is injected into the core-holder to reach the experimental pressure and then soak is allowed for 10 hours. After the soak period, we displace the soak gas with fresh gas and the produced oil is collected, which is defined as the production cycle. This process is repeated until no more oil is produced out from the core plugs, and the ultimate oil recovery can be calculated based on original oil in place. Further details are available from our previous publications (Adel et al. 2018a; Tovar et al. 2018a, b).

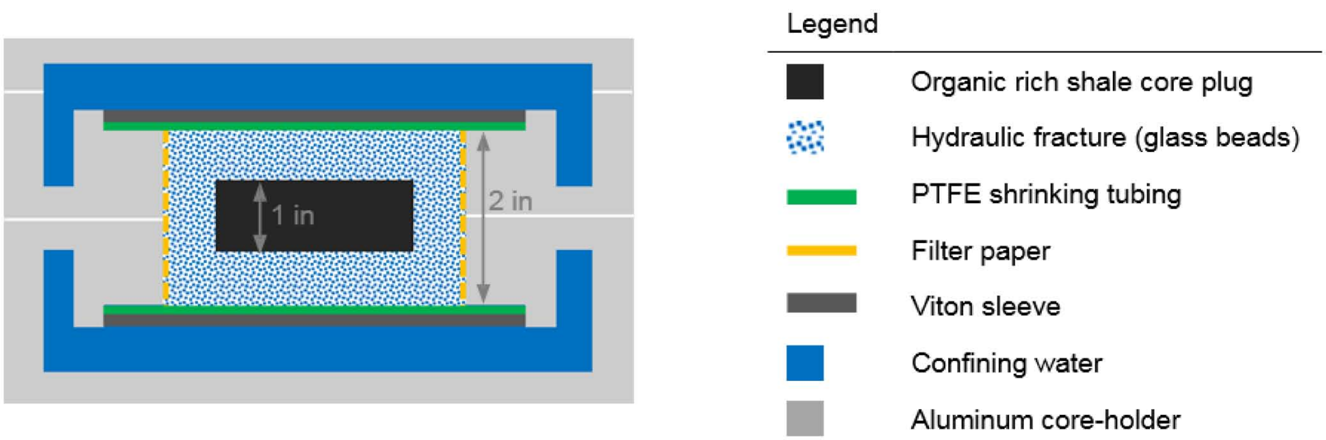

Figure 1—Schematic of the core-holder to physical simulate hydraulic fracture in the unconventional liquid reservoir (Adel et al. 2018a)

All core plugs were cleaned and re-saturated following a robust core preparation and re-saturation workflow. The cores are cleaned using the Dean and Stark methodology and then dried under vacuum over for two weeks. The core plugs were then re-saturated using their corresponding oil under 10,000 psi for three months. The objective of this core preparation procedure is to restore the cores to their original reservoir conditions, while accurately knowing estimating the OOIP.

The MMP is the minimum pressure at which the injected gas becomes miscible with oil, this is the most critical parameter during gas injection EOR. The injection pressure needs to be beyond the MMP to trigger the full potential of gas injection EOR. The slim tube method is considered the most accurate method to measure the MMP. We determined the MMP of CO_2- Eagle Ford oil system using slim tube method. Further details of the slim tube method to determine MMP are available in (Adel et al. 2016). In addition, the results of the MMP measurements are used to validate PVT table for the core-scale simulation.

Ternary Diagram

Ternary diagrams are used to analyze the mechanisms of CO_2 EOR during the injection process. Due to the multi-components of the oil sample, we construct a pseudo-ternary diagram to represent the oil we used in this study. Composition of the reservoir oil sample was determined using high resolution Gas Chromatography. We lumped oil compositions into two pseudo-component groups, which are intermediate components and heavy components. Equations of state (EOS) can be applied to calculate the Pressure-Volume-Temperature (PVT) of the gas/liquid equilibrium system (Rathmell et al. 1971).

In this study, we used Peng-Robinson EOS to construct the pseudo-ternary diagram for the CO_2-oil system. The workflow of the pseudo-ternary diagram construction is presented in Fig. 2. Properties of the pseudo-components were achieved from grouping the original composition of the oil sample.

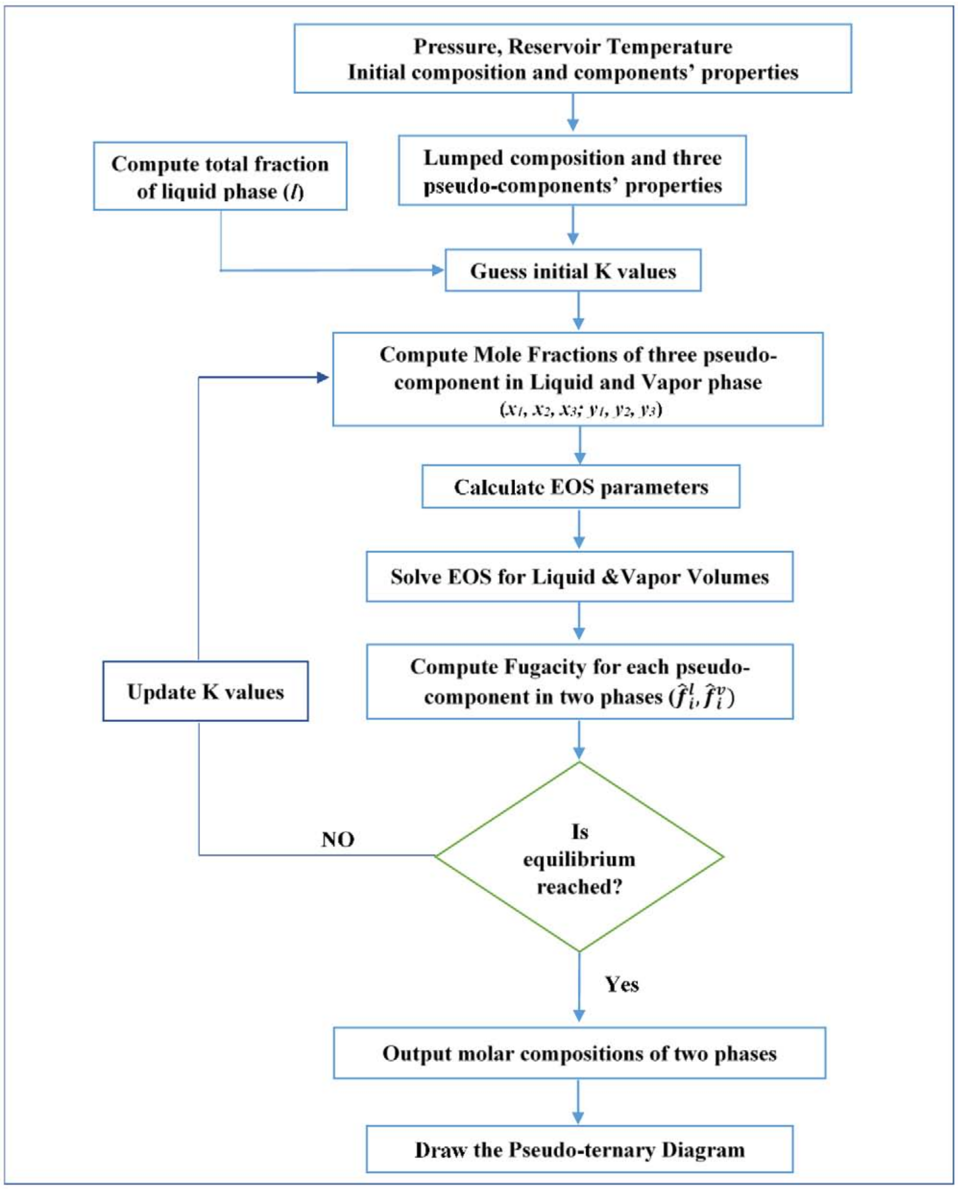

Figure 2—Workflow for the construction of the Pseudo-ternary Diagram

The binary interaction parameter for each component pairs is estimated using empirical equation Eq. 1, where V_{ci} and V_{cj} are critical molar volumes for component i and j, and θ is the exponential coefficient that is selected as Eq. 3 (Barragan et al. 2002).

$$k_{ij} = 1 - \left(\frac{2 * \left(V_{ci} * V_{cj} \right)^{\frac{1}{6}}}{V_{ci}^{\frac{1}{3}} + V_{cj}^{\frac{1}{3}}} \right)^{\theta} \tag{1}$$

The initial K-values for EOS calculation are estimated using Wilson's Equation (Wilson 1969), which is presented in Eq. 2. The K-value is a critical indicator for the solubility of CO_2 in oil.

$$K_i = \frac{y_i}{x_i} = \frac{P_{ci}}{P} \exp\left[5.37 (1 + w_i) \left(1 - \frac{T_{ci}}{T} \right) \right] \tag{2}$$

Where, x_i and y_i are the liquid and gaseous mole fractions of a component with index i. P_{ci} and T_{ci} are the critical pressure and temperature of component i. w_i is the acentric factor of the component.

The mixture is then flashed to obtain vapor and liquid compositions. Fugacity coefficients for each component were calculated using EOS when the liquid and vapor volumes were determined. The system equilibrium was determined by convergence of liquid and vapor fugacity. For each time step, a new K value can be calculated using Eq.3.

$$(K_i)^{k+1} = \left(\frac{\hat{f}_i^{\,l}}{\hat{f}_i^{\,v}} K_i \right)^{k} \tag{3}$$

Where, $\hat{f}_i^{\,l}$ and $\hat{f}_i^{\,v}$ are liquid and vapor fugacity of component i. k is the number of iteration step.

Core-Scale Model

The core-scale model was constructed using CT-scan technology to capture the heterogeneity of shale cores. CT number has a linear correlation with density, which means that higher CT number results in larger density. To accurately demonstrate the heterogeneity of the core plugs, we assigned different porosity and permeability value for each grid block. The porosity and permeability of each grid block are calculated from the CT number. The dimensions of the core-scale model, injection pressure, and soak time are precisely the same as the gas injection experiments.

The mechanisms of gas injection EOR are multi-contact miscibility and diffusion. We adjusted the related parameters to history match laboratory data using the core scale model. Diffusion coefficient of CO_2 at different pressure is determined from history matching laboratory data. Unfortunately, the diffusion coefficient is the only available parameter that can be tuned in the commercial simulator. To reveal the actual dominant mechanism of gas injection EOR, we compare the diffusion coefficient achieved from simulation to the diffusion coefficient measured in the laboratory. Typically, the diffusion coefficient has a positive linear trend with pressure.

Field-Scale Model

The large-scale field model was generated considering hydraulic fracturing simulation results, laboratory experiments, and core-scale simulation results. Diffusion coefficient achieved from core-scale history matching is implemented in the field model to present the effect of gas injection EOR. We used mixed gridding structure to construct the grid system of the field scale model. The grids surrounding and the ones inside the hydraulic fractures are equal size small grids, and the grids far from hydraulic fractures follow the logarithmic distribution. To decrease simulation error, the ratio between adjacent grids is less than 1.5. This gridding system not only increases the calculation speed but also guarantee the accuracy of the simulation results.

Since oil and water production from each stage is almost the same, two adjacent stages out of 14 stages were constructed to represent the whole well. The dimensions of this cropped reservoir model are 600 ft long, 1,600 ft wide, and 100 ft thick with a fracture half-length of 500 ft along the Y direction. Production data was normalized and allocated correspondingly as a target for the history matching process. We validated the field scale model by history match actual production data. The other parameters (such as permeability, porosity, fracture spacing, water saturation, etc.) are determined from history match results. The potential of CO_2 injection process in enhancing oil recovery in the unconventional liquid reservoir is evaluated using the field scale model. Further details regarding field-scale model construction are available in (Zhang et al. 2019a; Zhang et al. 2019b).

Results and Discussion

In this section, laboratory experiments results, ternary diagram analysis, core-scale history match, and field-scale simulation results are presented and discussed to reveal the actual dominant mechanism of gas injection EOR in unconventional reservoirs. Five different pressures are tested for CO_2 huff-n-puff experiments. The gas injection experiments were performed following a robust experiment workflow, and the soak time and production period for each cycle are 10 hours and 3 hours respectively.

Laboratory Experimental Results

Five experiments using re-saturated Eagle Ford cores were performed at different pressures at reservoir temperature. All the gas injection experiments were set up inside the CT scanner to guarantee the CT image to represent the same exact position/slice at each time. Soak and production times for each cycle are maintained constant at 10 hours and 3 hours respectively. The experimental pressures varied from 1,400 psi to 3,500 psi.

The MMP is a critical parameter for any gas injection EOR design. The injection pressure needs to be higher than the MMP to trigger the multi-contact miscibility effect. Multi-contact miscibility is the primary mechanism for gas injection EOR. We measured the MMP using the slim-tube method, which is the most accurate method to determine the MMP. For this Eagle Ford oil, the MMP is determined to be 2,130 psi. Further details regarding the slim tube method are available in (Adel et al. 2018a).

Five CO_2 Huff-n-Puff experiments were performed at reservoir temperature. Two experimental pressures are below the MMP, which are 1,400 psi and 1,800 psi. The other pressures are above the MMP, which are 2,500 psi, 3,000 psi, and 3,500 psi. The ultimate oil recovery for all gas injection experiments is presented in Fig. 3. The highest recovery factor is 49% (OOIP), which was achieved from the gas injection experiments at 3,500 psi. However, the recovery factors are less than 5% when the pressure below the MMP.

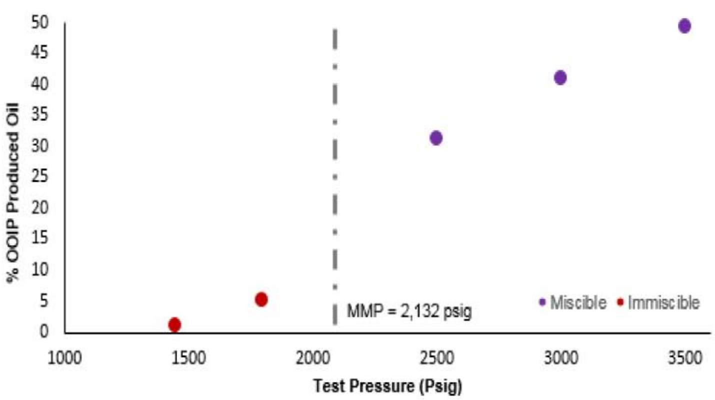

Miscibility Status	Test Pressure (psig)	Oil Recovery (% of OOIP)
Miscible	3500	49.31
	3000	40.9
	2500	31.03
Immiscible	1800	5.00
	1450	1.00
Res Temp (°F)	170	
MMP (psig)	2,132	

Figure 3—Ultimate recovery factors for gas injection experiments at different pressure

Increasing pressure always results in higher ultimate oil recovery, especially when the pressure is beyond the MMP. In conventional reservoirs however, reaching the MMP is enough to attain the highest recovery factors. These results challenge the paradigm that operating slightly above the MMP is the optimum injection pressure for EOR designs. Increasing the injection pressure leads to better oil production enhancement in the unconventional liquid reservoirs. In the following section, we used a ternary diagram analysis method to explain this relationship between pressure and recovery factor.

Ternary Diagram Analysis

The ternary diagram is commonly utilized to demonstrate the miscibility process, which is a dynamic fluid mixing and component exchange process. In most of gas injection processes, gas-oil miscibility is achieved through the multi-contact process. In this study, we demonstrate the multi-contact miscibility process using a ternary diagram, then analyze the effect of pressure on miscibility process. Finally, we discuss the correlation between pressure and recovery factor in shale reservoir using ternary diagram analysis results.

The ternary diagram for miscibility and production processes during gas injection experiment is presented in Fig. 4. As gas is injected to cylinder and contacted with oil, the mixture point of injection gas and crude oil lying in the two-phase area. The location of the mixture is determined by the volume proportion of oil and gas, which is shown as O_1 and G_1. Then, the gas continues contacting with reservoir oil and mixed into the oil phase. The new mixture point moves to M_2, O_2 and G_2 which are the corresponding oil and gas fractions at M_2 state. This process repeatedly happens until reaching the critical point where the gas and oil are miscible.

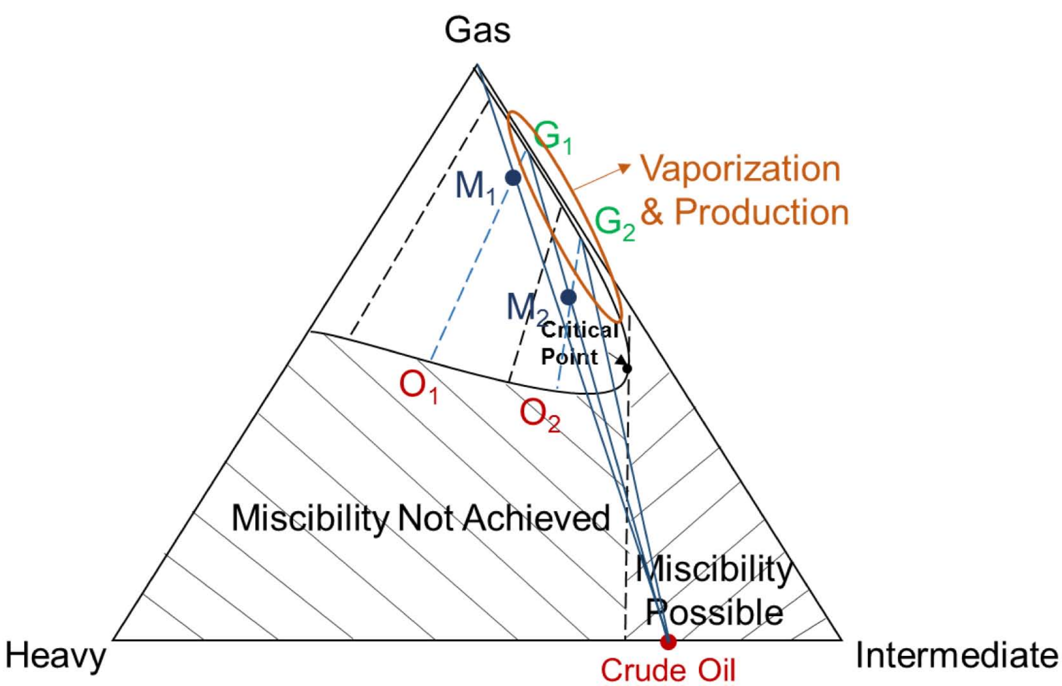

Figure 4—Schematic of the ternary diagram for the determination of miscibility and production processes during gas injection experiment

Only the original oil composition located in the ‘miscibility possible’ zone shown in Figure 4, can move to the critical point in the end. Therefore, multi-contact miscibility is achieved through the multi-contact process. Otherwise, the original oil composition is located in the ‘miscibility not achieved’ zone, and the extension of a tie line (such as the G2-O2 line) passes through the oil. The multi-contact process is suspended at this point and the miscibility state cannot be achieved.

As pressure increases, the two-phase area shrinks and the critical tie line moves towards to the gas-heavy components side. According to its definition, minimum miscibility pressure occurs when the critical tie line first intersects the crude oil point in the ternary diagram. We can estimate the MMP numerically using ternary diagrams, but this method needs to be validated by slim tube laboratory data.

In the multi-contact process, intermediate components of the oil phase vaporize into the gas phase, and gas dissolves into the oil phase. This dynamic process primarily happens in the soak period during the gas injection experiment. The vaporized oil, along with gas, is produced during the production period and condenses back to liquid phase at room pressure and temperature. During the gas injection experiment, oil is produced through the vaporization and condensation drive.

The two-phase area bounded by the bubble curve and dew curve shrinks as pressure increases. The critical tie line moves towards the gas-heavy component side, which indicates that miscibility occurs at higher pressures. In order to demonstrate the effect of pressure on improving recovery factor, we plotted the ternary diagrams for different pressures in the same figure. Figure 5 is the merged ternary diagram for the Eagle Ford oil at different pressures. The original oil composition located in zone A can reach miscibility representing the experimental pressure at 2,500 psi. As pressure increases to 3,000 psi, the oil composition located in zone B can achieve miscibility state. Further increase pressure, a broader spectrum of oil can reach miscibility with CO_2.

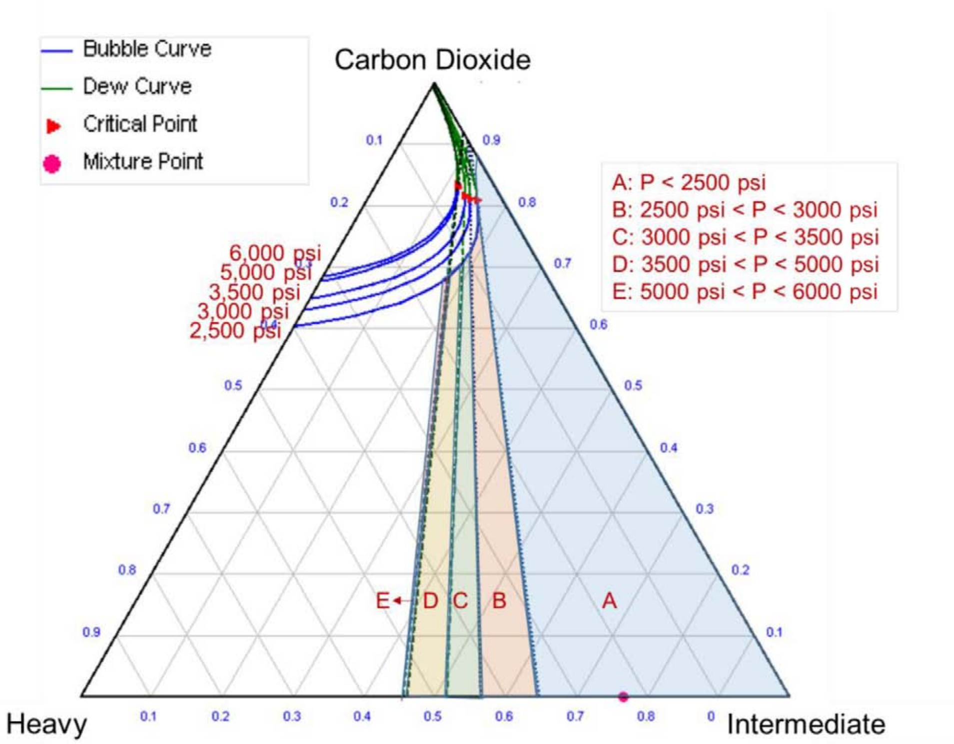

Figure 5—Ternary diagram for Eagle Ford oil sample at different pressure

The heterogeneity nature of unconventional reservoir rock results in a widespread pore size distribution. Due to confinement of smaller pores, the heavy components of the oil have the tendency to concentrate in small radius pores. The MMP determined from slim tube experiment is the miscibility pressure for the general composition of oil with gas. Actually, oil within the small pores possesses a higher MMP compared to the MMP measured using slim tube method. Due to the heterogeneity pore size in shale rock, the MMP for the specific pore radius can be varied from 2,000 psi to 5,000 psi.

During CO_2 Huff-n-Puff experiment, increasing experimental pressure results in a higher oil recovery due to the additional oil in the smaller pore being able to reach miscibility. We also observed the color of produced oil from gas injection experiments becoming darker as pressure increases. Based on these observations, further increase in pressure beyond the MMP leads to larger oil production enhancement. However, there is an optimum injection pressure for gas injection EOR. In this study, most of the oil reaches miscibility when the pressure at 5,000 psi. Further increasing pressure does not result in a significant oil production enhancement, especially the injection pressure above 5,000 psi.

Core-Scale History Match

To reveal the mechanisms of gas injection EOR and upscale the experimental data to the field scale, we determine the parameters that govern the gas injection EOR process from history matching the experimental results utilizing a core-scale model. A slim tube model was constructed and history matched with the MMP data to achieve an accurate PVT table for the core-scale simulation model. We then developed the core-scale model by combining CT-scan technology, laboratory data, and slim-tube history matching results. Finally, we history match the gas injection experimental data to obtain the diffusion coefficient of CO_2 and discuss the primary mechanism of gas injection EOR from the core-scale simulation results.

It is essential to utilize an accurate PVT table to history match the gas injection experiment results and to estimate the diffusion coefficient. We validated the PVT table by combining the history match of the slim tube MMP data and the Gas Chromatography (GC) results. The slim tube simulation model was constructed considering the geometries and properties of the slim-tube used in laboratory experiments. The injection rate and injection pressure are also consistent with MMP experiment. Phase behavior of each component in the oil composition is mainly controlled by its *k-value* in the PVT table. The *K-value* table was adjusted to match our experimental results. We history match the Eagle Ford MMP data using a numerical simulation model, and the results are presented in Fig. 6.

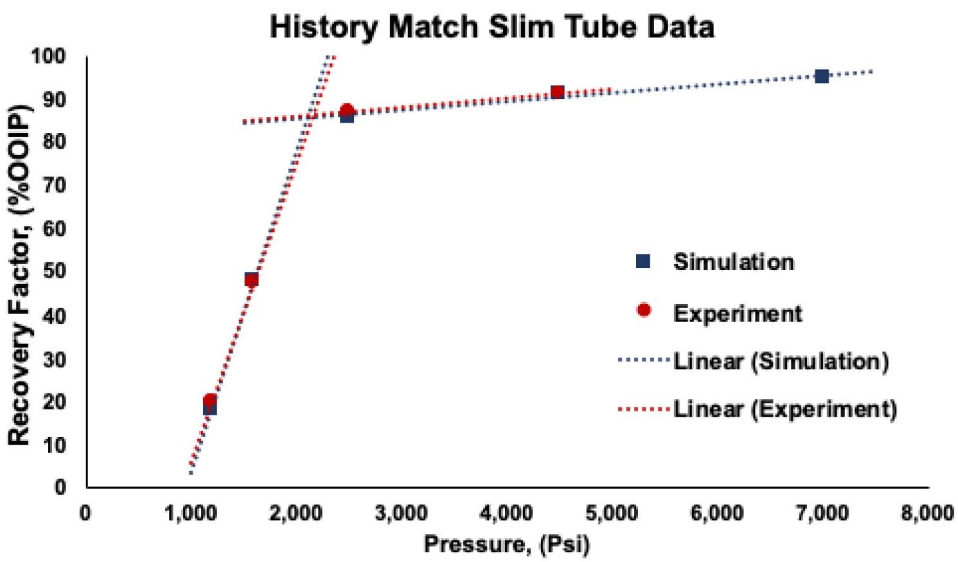

Figure 6—History match slim tube MMP data

Fig. 6 demonstrates that the simulation results have a good agreement with the experimental results. The consistency of simulation results with experimental results indicates the PVT table is credible. Since the parameters of the slim tube simulation model are the same as laboratory experiments, the corresponding PVT table for this history match result is used to represent the oil in MMP measurements. This PVT table will be implemented in the core-scale simulation model to determine the diffusion coefficient of CO_2, which is utilized in the field-scale model to evaluate the potential of gas injection EOR in the unconventional liquid reservoirs.

The core-scale model is constructed using CT scan technology to represent the heterogeneity of the core plugs. We converted the CT number to porosity and permeability for each grid block to distinguish the bedding planes of the tight rock. Comparison of actual core images (CT image) and converted core-scale structures is shown in Fig. 7.

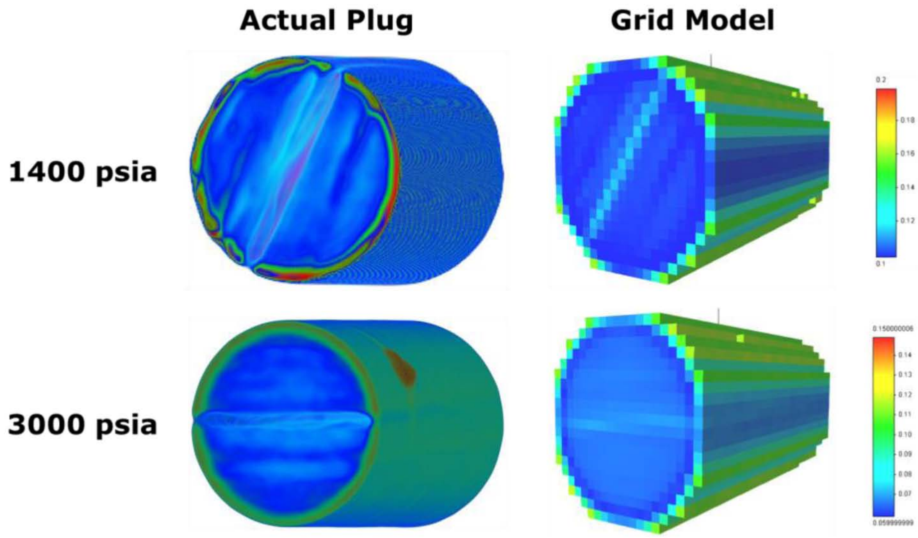

Figure 7—Comparison of the 3D CT-scan image (left) and core-scale model (right)

In Fig. 7, we show the core plugs used in the gas injection experiments at 1,400 psi and 3,000 psi. Due to the highly heterogeneity nature of the shale cores, it is essential to integrate heterogeneity into the core model to ensure the accuracy of estimating the diffusion coefficient at different pressures. Fig. 7 indicates the core-scale model has successfully captured the heterogeneity of the core plugs, especially the bedding planes of the core plugs.

The initial condition of the core-scale model was established to present the laboratory conditions accurately. The core plug grid model shown in Fig. 7 was placed in the center of the core-scale model and surrounded by high permeability region which is used to represent the glass beads. The initial pressure of 1,000 psi, the soak time of 10 hours, and the productions time of 3 hours for each cycle, are all consistent with the laboratory experiments. Previously, the PVT table for the Eagle Ford oil was estimated by combining the slim tube history match results and the GC report of oil composition. We implemented this PVT table in our core-scale model and history match the gas injection experiments at different pressures. The history match results of gas injection experiments using the core-scale model are presented in Fig. 8

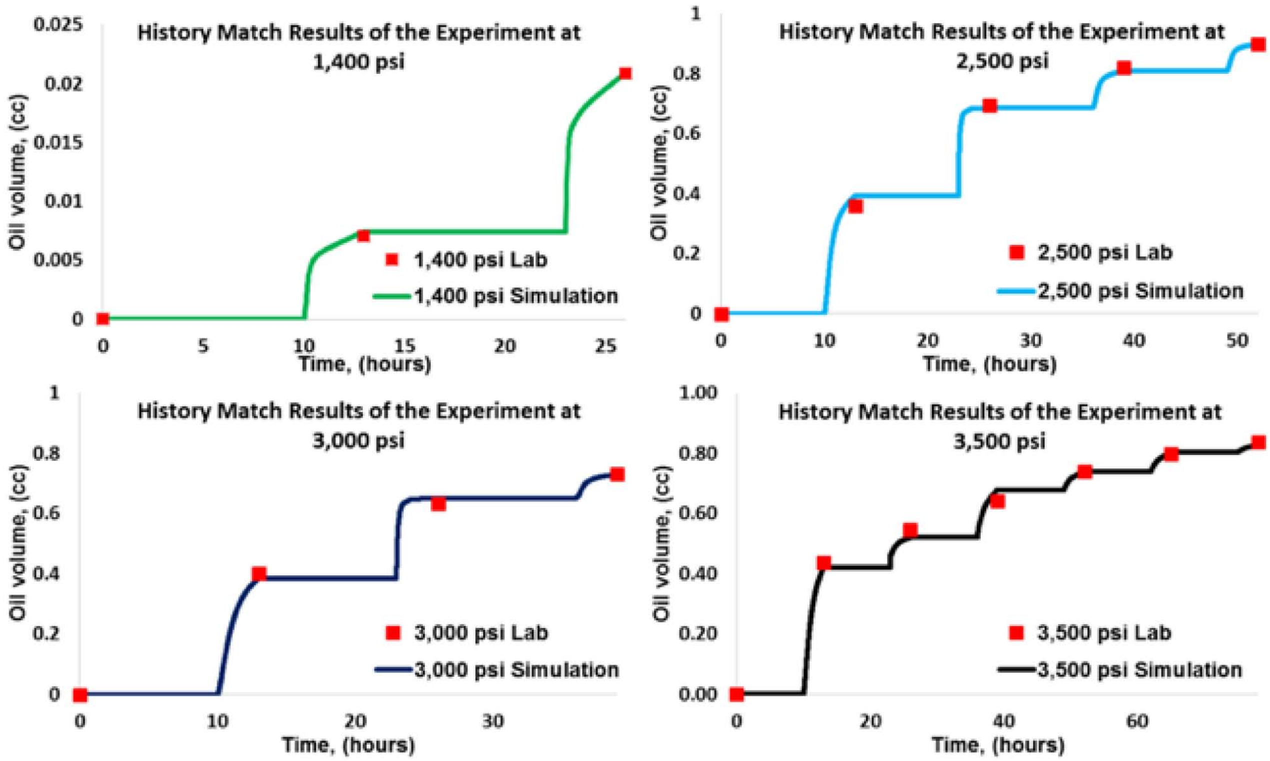

Figure 8—The history-matching results of gas injection experiments at different pressure

Fig. 8 demonstrates that the history match results have a decent agreement with the experimental results for all gas injection experiments. Since the diffusion coefficient is the only parameter that can be utilized to tune the gas injection EOR effect in the simulator, we plotted the diffusion coefficient of CO_2 from history matching results in Fig. 9 to analyze the effect of diffusion.

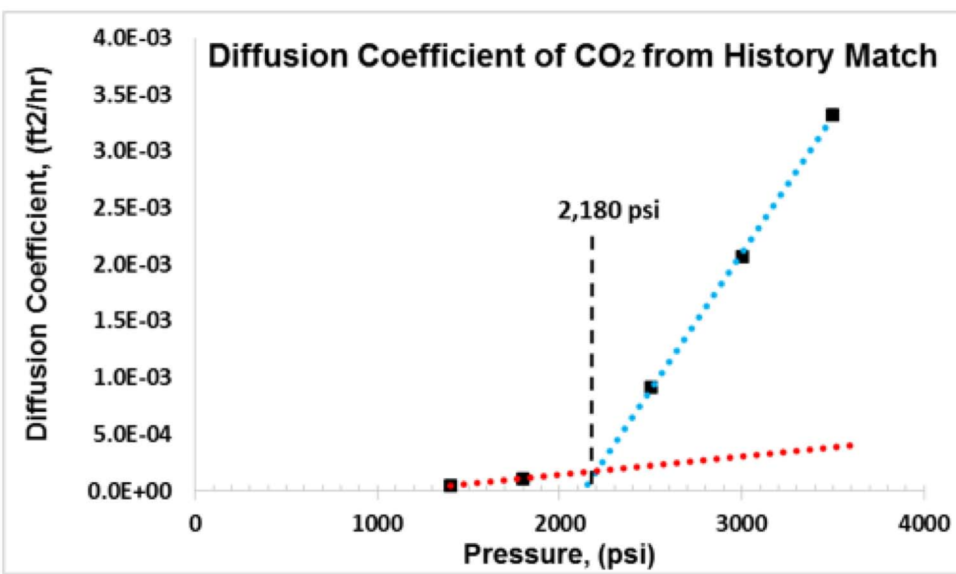

Figure 9—The diffusion coefficient of CO_2 from history matching results

Fig. 9 illustrates that the history match diffusion coefficient separates into two groups, which are high pressure group and low pressure group (below the MMP). The diffusion coefficient in each group has a linear correlation with pressure, and the intersection of these two trend lines at 2,180 psi, which is close to the MMP. It is an exciting finding that miscibility presented a significant influence of gas injection EOR effect. In addition, the diffusion coefficient of CO_2 from history match results for the experiments performed below the MMP is much smaller than the diffusion coefficient for the experiments beyond the MMP. The diffusion coefficient of CO_2 for the group of above the MMP is larger by two orders of magnitude to the diffusion coefficient for the group below the MMP. However, from the literature, the diffusion coefficient of CO_2 should only be in positive linear trend with pressure, which is not consistent with history match results. The actual effect of diffusion for gas injection EOR is along the red line, which plays a minor role in gas injection EOR. The difference between to blue line and the red line is the effect of the multi-contact miscibility. Due to the fact that diffusion coefficient is the only parameter that can be tuned in the simulator, the diffusion coefficients from history matching results is the combined effect of miscibility and diffusion. Based on the observations from the core-scale simulation results and ternary diagram analysis, the actual dominant mechanism of gas injection EOR is the multi-contact miscibility effect.

An additional laboratory observation that also provides evidence that diffusion possesses a less oil production enhancement effect than multi-contact miscibility. We performed gas injection experiment using N_2 following the same procedure as the gas injection experiment presented in this paper. Although the pressure of N_2 injection experiments increased to 5,000 psi, oil in the shale core plugs still cannot be produced out from matrix. The multi-contact miscibility effect on improving oil recovery cannot be triggered since to the MMP of oil-N_2 is very high (higher than 5,000 psi). However, the diffusion coefficient of N_2 at 5,000 psi is the same order of magnitude to the diffusion coefficient of CO_2. Based on this observation, the primary mechanism of gas injection EOR is multi-contact miscibility and diffusion play a minor role in improving oil recovery in unconventional liquid reservoirs.

CO_2 Injection EOR Application Using the Field-Scale

The field-scale model was developed by following a comprehensive workflow, which consists of combining the laboratory data, the core-scale history match results, and the hydraulic fracturing simulation results. Two adjacent hydraulic fractures stages were randomly selected to construct the field scale model, which is presented in Fig. 10. The dimensions of the field-scale model are 600 ft, 1,600 ft, and 100 ft with a mixed gridding structure to ensure the accuracy of simulation results and to decrease the simulation time. Five hydraulic fracture clusters are generated in each stage, in which two or three hydraulic fracture clusters were suppressed by the pressure shadow effect from adjacent clusters and stages. In reality, this stress shadowing effect is also observed in the field as some of the clusters grow short and narrow. Due to the large number of natural fractures existing in unconventional liquid reservoirs and the fact that the permeability of the matrix is ultra-low, we constructed the reservoir simulation model using a dual-porosity system.

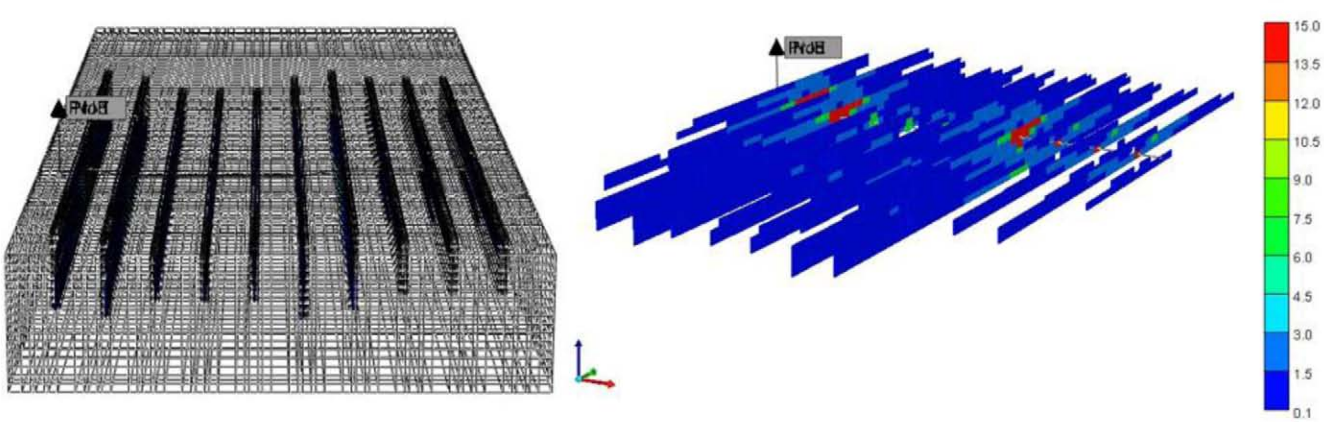

Figure 10—Gridding structure (left) and permeability distribution in hydraulic fractures of the field-scale.

The field-scale model was validated by history matching the actual well production data. Porosity, permeability, and water saturation for both fracture and matrix system as well as fracture spacing were tuned to history match the well production data. The best history match results of cumulative oil and water production are presented in Fig. 11, and all the reservoir properties can be determined from the history match results.

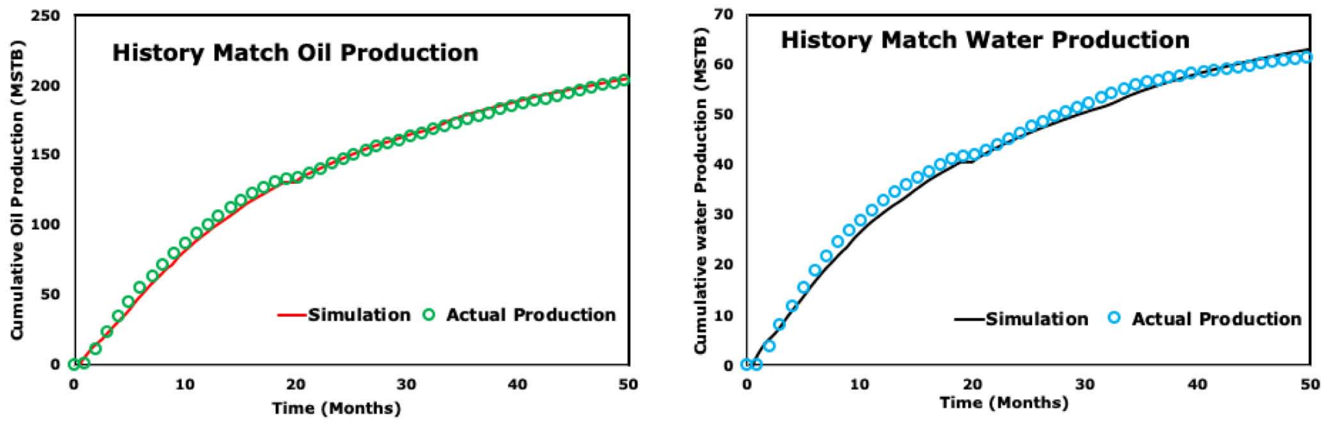

Figure 11—The history match results of the field-scale model to the actual oil (left) and water (right) production data

Both cumulative oil and water production from simulation results have a decent agreement with the actual well production data. The error of the history match in the cumulative oil and water production is less than 1%; this indicates that the field-scale model is representative of the actual reservoir conditions. The field-scale model could provide convincing simulation results for investigating different EOR applications. After validating the field-scale model, gas huff-n-puff EOR is evaluated using the validated field-scale model.

The results of the gas injection experiments prove the potential of gas injection as an effective EOR technique in improving oil recovery in unconventional liquid reservoirs. In order to evaluate the effectiveness of gas injection EOR, we studied the oil production enhancement through numerical simulation using validated field-scale model. The diffusion coefficient achieved from the core-scale history match was implemented in the field-scale model. In this study, we tested the effect of injection pressure on improving oil recovery and compared it to the base case that is the best history match case. In addition to the injection pressure, the start time of gas injection treatment was also investigated to observe the effect on oil production enhancement. Cumulative oil production was picked as the primary factor to demonstrate the performance of the gas injection process. The incremental recovery was calculated as follow: (cumulative oil production of gas injection case - cumulative oil production of the base case)/ cumulative oil production of the base case.

Two injection pressures (4,000 psi and 4,500 psi) were tested to demonstrate the effect of injection pressure. The cumulative oil production and incremental recovery for both cases are presented in Fig. 12. The incremental recovery is determined by comparing the recovery factor to that of the base case. Fig. 12 indicates that the gas injection process after primary depletion results in oil production enhancement. In addition, the higher the injection pressure leads to more oil production from the reservoir, which is consistent with the laboratory results. Higher injection pressure not only causes more oil to reach a miscible state with the gas, but also builds up the reservoir pressure. During the depletion process, oil production is determined by the pressure difference. Due to this fact, re-energizing the reservoir to a higher pressure can improve oil production. Both effects lead to an increase oil production during the gas injection process.

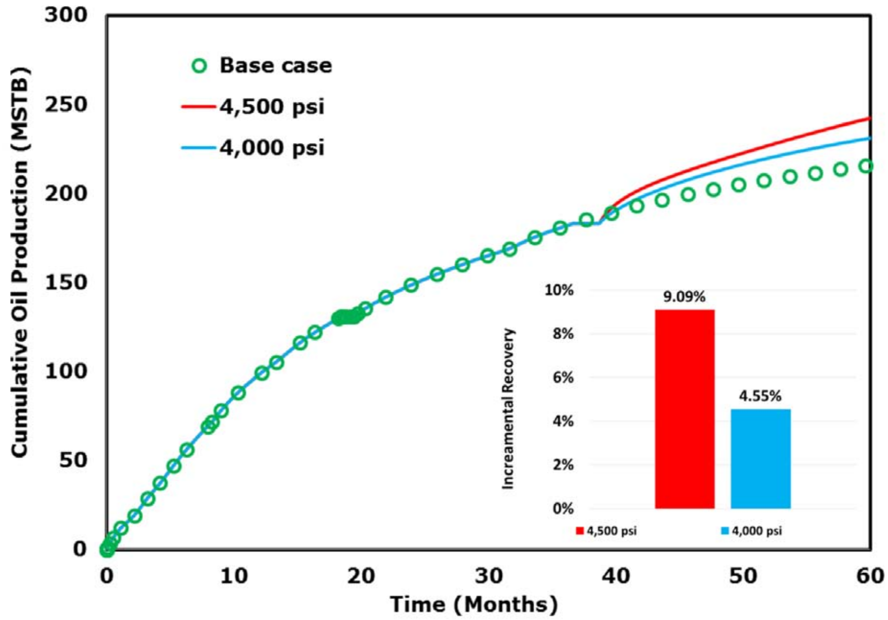

Figure 12—Simulation results of cumulative oil production and recovery incremental for different injection pressure

The impact of the start time of the gas injection process is then investigated, and the simulation results are shown in Fig. 13. We tested two gas injection start times at 4,500 psi, which are three and four years after oil production. The gas injection start time does not show a strong effect on oil production enhancement when compared to the effect of injection pressure. Gas injection process starting after three years production leads to a slightly better performance than the four-year case. In addition, the start time of gas injection should not be less than two years. Due to the limitation of injection pressure, it is difficult to inject enough gas volume into reservoir to economically improve oil production in unconventional liquid reservoirs. In this study, three years is found to be the optimum gas injection start time.

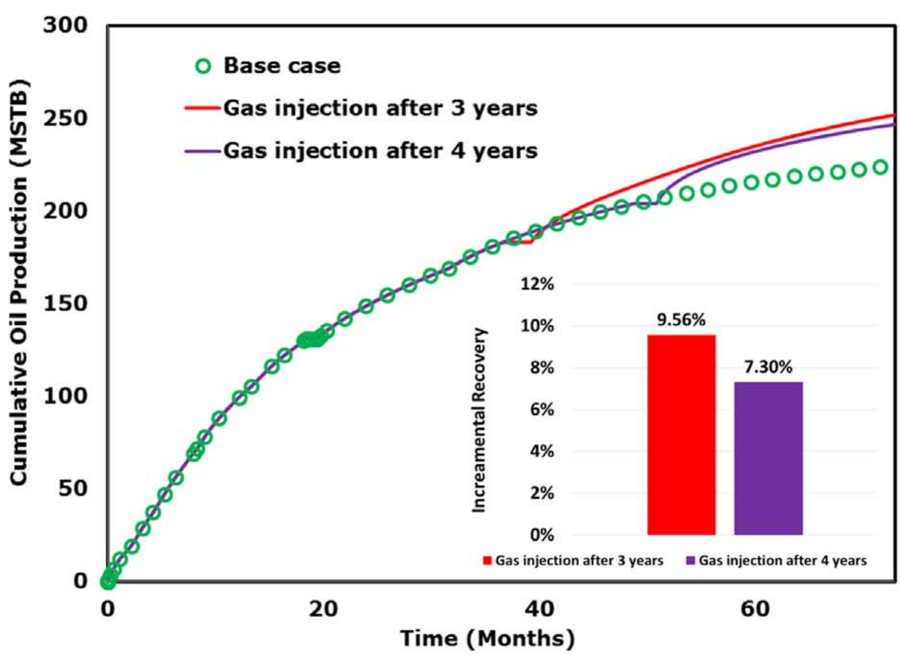

Figure 13—Simulation results of cumulative oil production and recovery incremental for the different gas injection start time

Conclusion

Based on the observations from laboratory data, ternary diagram analysis, and numerical simulation results for a specific Eagle Ford well, we conclude:

1. CO_2 injection EOR in unconventional liquid reservoirs through hydraulic fractures results in higher oil production. This gas EOR effect is observed in the laboratory experiments and numerical simulation results.
2. The MMP is the most critical parameter for gas injection EOR; the injection pressure should be higher than the MMP to achieve a significant oil production enhancement.
3. Increasing pressure always leads to higher oil recovery, especially when operating above the MMP. This phenomenon was observed in the gas injection experiments and explained through ternary diagram analysis.
4. The mechanisms of gas injection EOR are multi-contact miscibility, diffusion, and vaporization-condensation gas drive, which is demonstrated from ternary diagram analysis and core-scale simulation results.
5. The dominant mechanism of gas injection EOR is multi-contact miscibility, while diffusion plays a minor role. The actual contribution of diffusion effect for enhancing oil recovery is along the red trend line in Fig. 9, which consists of a lesser portion of the oil production enhancement when compared to contribution of the multi-contact miscibility drive.
6. Gas injection is a feasible EOR technique to enhance oil recovery in unconventional liquid reservoirs.

Acknowledgments

The authors would like to show their appreciation to the staff and student worker at the Petroleum Engineering Department at Texas A&M University for their collaboration on the laboratory work and data collection. The authors are thankful to Crisman Institute for Petroleum Research at Texas A&M University, Halliburton, Marathon Oil, Chevron, Pioneer Natural Resources for providing equipment or funding this project.

Nomenclature

V_{ci} = Critical molar volumes for component i
V^{cj} = Critical molar volumes for component j
$\hat{f}_i^l$ = Liquid fugacity of component i
$\hat{f}_i^v$ = Vapor fugacity of component i
k_{ij} = Binary interaction parameter
k = Number of iteration
K_i = K value for EOS
P_{ci} = Critical capillary pressure of component i
P = Pressure
T_{ci} = Critical temperature of component i
T = Temperature
w_i = Acentric factor of component i
x_i = Liquid mole fractions of a component with index i
y_i = Gaseous mole fractions of a component with index
θ = Exponential coefficient
CT = Computed tomography
EOR = Enhanced oil recovery

EOS = Equation of state
GC = Gas Chromatography
MMP =Minimum miscibility pressure
OOIP = Original oil in place
PVT = Pressure-Volume-Temperature
ULR = Unconventional Liquid Reservoir

Reference

Adel, I.A., Tovar, F.D., and Schechter, D.S. (2016). Fast-Slim Tube: A Reliable and Rapid Technique for the Laboratory Determination of Mmp in CO2 - Light Crude Oil Systems. Presented at the SPE Improved Oil Recovery Conference, Tulsa, Oklahoma, USA. https://doi.org/10.2118/179673-ms.

Adel, I.A., Tovar, F.D., Zhang, F. et al. 2018a. The Impact of Mmp on Recovery Factor During CO2 – EOR in Unconventional Liquid Reservoirs. Presented at the SPE Annual Technical Conference and Exhibition, Dallas, Texas, USA. 17. https://doi.org/10.2118/191752-MS.

Adel, I.A., Zhang, F., Bhatnagar, N. et al. 2018b. The Impact of Gas-Assisted Gravity Drainage on Operating Pressure in a Miscible CO2 Flood. Presented at the SPE Improved Oil Recovery Conference, Tulsa, Oklahoma, USA. https://doi.org/10.2118/190183-ms.

Afra, S., Nasr-El-Din, H.A., and Samouei, H. 2019a. Characterization of Iron Interaction with Viscoelastic Surfactant (Ves)-Based Stimulation Fluid. Presented at the SPE Western Regional Meeting, San Jose, CA, USA. https://doi.org/10.2118/195373-ms.

Afra, S., Nasr-El-Din, H.A., Socci, D. et al. 2018. Green Phenolic Amphiphile as a Viscosity Modifier and Asphaltenes Dispersant for Heavy and Extra-Heavy Oil. *Fuel* **220**: 481–489. https://doi.org/10.1016/j.fuel.2018.01.111.

Afra, S., Samouei, H., and Nasr-El-Din, H.A. 2019b. Characterization of Iron Interaction with Viscoelastic Surfactant Ves-Based Stimulation Fluid. Presented at the SPE Middle East Oil and Gas Show and Conference, Manama, Bahrain. 10. 10.2118/194862-MS.

Alhashim, H., W, Zhang, F., and Schechter, D.S. (2019). Investigation of the Effect of Pore Size Distribution on the Produced Oil from Surfactant-Assisted Spontaneous Imbibition in Ulr Using Nmr. Presented at the SPE Annual Technical Conference and Exhibition, Calgary, Albert, Canada. https://doi.org/10.2118/195931-MS

Alvarez, J.O., Saputra, I.W.R., and Schechter, D.S. (2018). The Impact of Surfactant Imbibition and Adsorption for Improving Oil Recovery in the Wolfcamp and Eagle Ford Reservoirs. *SPE Journal* **23** (06): 2103–2117. SPE-187176-PA. 10.2118/187176-PA.

Alvarez, J.O. and Schechter, D.S. (2017). Wettability Alteration and Spontaneous Imbibition in Unconventional Liquid Reservoirs by Surfactant Additives. *Spe Reservoir Evaluation & Engineering* **20** (1): 107–117. Spe Reserv Eval Eng. https://doi.org/10.2118/177057-Pa.

Bao, A. and Gildin, E. 2017. Data-Driven Model Reduction Based on Sparsity-Promoting Methods for Multiphase Flow in Porous Media. Presented at the SPE Latin America and Caribbean Petroleum Engineering Conference, Buenos Aires, Argentina. 16. https://doi.org/10.2118/185514-MS.

Bao, A., Hazlett, R.D., and Babu, D.K. (2017). A Discrete, Arbitrarily Oriented 3d Plane-Source Analytical Solution to the Diffusivity Equation for Modeling Reservoir Fluid Flow. *SPE Journal* **22** (05): 1609–1623. SPE-185180-PA. https://doi.org/10.2118/185180-PA.

Barragan, M., Woods, S., Julien, H.L. et al. 2002. Thermodynamic Equations of State for Hydrazine and Monomethylhydrazine. *Combustion and Flame* **131** (3): 316–328. https://doi.org/10.1016/S0010-2180(02)00410-8.

Deng, L. and King, M.J. (2015). Capillary Corrections to Buckley-Leverett Flow. Presented at the SPE Annual Technical Conference and Exhibition, Houston, Texas, USA. https://doi.org/10.2118/175150-ms.

Deng, L. and King, M.J. (2018). Theoretical Investigation of the Transition from Spontaneous to Forced Imbibition. Presented at the SPE Improved Oil Recovery Conference, Tulsa, Oklahoma, USA. https://doi.org/10.2118/190309-ms.

Hoffman, B.T. (2012). Comparison of Various Gases for Enhanced Recovery from Shale Oil Reservoirs. Presented at the SPE Improved Oil Recovery Symposium, Tulsa, Oklahoma, USA. 8. 10.2118/154329-MS.

Kou, R., Moridis, G.J., and Blasingame, T.A. (2018). Analysis and Modeling of Proppant Transport in Inclined Hydraulic Fractures. Presented at the SPE Hydraulic Fracturing Technology Conference and Exhibition, The Woodlands, Texas, USA. https://doi.org/10.2118/189856-ms.

Kumar, A., Gohary, M.E., Pedersen, K.S. et al. 2015. Gas Injection as an Enhanced Recovery Technique for Gas Condensates. A Comparison of Three Injection Gases. Presented at the Abu Dhabi International Petroleum Exhibition and Conference, Abu Dhabi, UAE. 13. 10.2118/177778-MS.

Pan, Y., Zhou, P., Deng, L. et al. 2019. Production Analysis and Forecasting for Unconventional Reservoirs Using Laplacian Echo-State Networks. Presented at the SPE Western Regional Meeting, San Jose, California, USA. 28. https://doi.org/10.2118/195243-MS.

Rathmell, J.J., Stalkup, F.I., and Hassinger, R.C. (1971). A Laboratory Investigation of Miscible Displacement by Carbon Dioxide. Presented at the Fall Meeting of the Society of Petroleum Engineers of AIME, New Orleans, Louisiana. 16. 10.2118/3483-MS.

Saputra, I.W.R. and Schechter, D.S. (2018). Comprehensive Workflow for Lab to Field-Scale Numerical Simulation to Improve Oil Recovery in the Eagle Ford Shale by Selective Testing and Modeling of Surfactants for Wettability Alteration. Presented at the SPE/AAPG/SEG Unconventional Resources Technology Conference, Houston, Texas, USA. https://doi.org/10.15530/urtec-2018-2884598.

Sun, J.L., Zou, A., Sotelo, E. et al. 2016. Numerical Simulation of CO2 Huff-N-Puff in Complex Fracture Networks of Unconventional Liquid Reservoirs. *Journal of Natural Gas Science and Engineering* **31**: 481–492. J Nat Gas Sci Eng. https://doi.org/10.1016/j.jngse.2016.03.032.

Tang, H., Killough, J.E., Heidari, Z. et al. 2017. A New Technique to Characterize Fracture Density by Use of Neutron Porosity Logs Enhanced by Electrically Transported Contrast Agents. *SPE Journal* **22** (04): 1034–1045. SPE-181509-PA. https://doi.org/10.2118/181509-PA.

Tang, H., Yan, B., Chai, Z. et al. 2018. Analyzing the Well-Interference Phenomenon in the Eagle Ford Shale/Austin Chalk Production System with a Comprehensive Compositional Reservoir Model. *SPE Reservoir Evaluation & Engineering* ***Preprint*** *(Preprint)*: 15. SPE-191381-PA. https://doi.org/10.2118/191381-PA.

Tovar, F.D., Barrufet, M.A., and Schechter, D.S. 2018a. Gas Injection for EOR in Organic Rich Shale. Part I: Operational Philosophy. Presented at the SPE Improved Oil Recovery Conference, Tulsa, Oklahoma, USA. https://doi.org/10.2118/190323-ms.

Tovar, F.D., Barrufet, M.A., and Schechter, D.S. 2018b. Gas Injection for EOR in Organic Rich Shales. Part Ii: Mechanisms of Recovery. Presented at the SPE/AAPG/SEG Unconventional Resources Technology Conference, Houston, Texas, USA. 21. 10.15530/URTEC-2018-2903026.

Wan, T., Sheng, J.J., and Soliman, M.Y. (2013). Evaluation of the EOR Potential in Shale Oil Reservoirs by Cyclic Gas Injection. Presented at the SPWLA 54th Annual Logging Symposium, New Orleans, Louisiana. 16.

Wilson, K.G. (1969). Non-Lagrangian Models of Current Algebra. *Physical Review* **179** (5): 1499–1512. 10.1103/PhysRev.179.1499.

Xue, X., Yang, C., Park, J. et al. 2018. Reservoir and Fracture-Flow Characterization Using Novel Diagnostic Plots. *SPE Journal* ***Preprint*** *(Preprint)*: 22. SPE-194017-PA. https://doi.org/10.2118/194017-PA.

Yang, C., Xue, X., Huang, J. et al. 2016. Rapid Refracturing Candidate Selection in Shale Reservoirs Using Drainage Volume and Instantaneous Recovery Ratio. Presented at the SPE/AAPG/SEG Unconventional Resources Technology Conference, San Antonio, Texas, USA. 16. https://doi.org/10.15530/URTEC-2016-2459368.

Yang, C., Xue, X., King, M.J. et al. 2017. Flow Simulation of Complex Fracture Systems with Unstructured Grids Using the Fast Marching Method. Presented at the SPE/AAPG/SEG Unconventional Resources Technology Conference, Austin, Texas, USA. 18. https://doi.org/10.15530/URTEC-2017-2691393.

Yang, D., Xue, X., and Chen, J. 2018. High Resolution Hydraulic Fracture Network Modeling Using Flexible Dual Porosity Dual Permeability Framework. Presented at the SPE Western Regional Meeting, Garden Grove, California, USA. 14. https://doi.org/10.2118/190096-MS.

Zhang, F., Adel, I.A., Park, K.H. et al. 2018a. Enhanced Oil Recovery in Unconventional Liquid Reservoir Using a Combination of CO2 Huff-N-Puff and Surfactant-Assisted Spontaneous Imbibition. Presented at the SPE Annual Technical Conference and Exhibition, Dallas, Texas, USA. 20. https://doi.org/10.2118/191502-MS

Zhang, F., Saputra, I.W.R., Adel, I.A. et al. 2018b. Scaling for Wettability Alteration Induced by the Addition of Surfactants in Completion Fluids: Surfactant Selection for Optimum Performance. Presented at the SPE/AAPG/SEG Unconventional Resources Technology Conference, Houston, Texas, USA. 17. https://doi.org/10.15530/URTEC-2018-2889308.

Zhang, F., Saputra, I.W.R., Adel, I.A. et al. 2019a. Numerical Investigation of EOR Applications in Unconventional Liquid Reservoirs through Surfactant-Assisted Spontaneous Imbibition (Sasi) and Gas Injection Following Primary Depletion. Presented at the SPE Annual Technical Conference and Exhibition, Calgary, Albert, Canada. https://doi.org/10.2118/196055-MS

Zhang, F., Saputra, I.W.R., Niu, G. et al. 2018c. Upscaling Laboratory Result of Surfactant-Assisted Spontaneous Imbibition to the Field Scale through Scaling Group Analysis, Numerical Simulation, and Discrete Fracture Network Model. Presented at the SPE Improved Oil Recovery Conference, Tulsa, Oklahoma, USA. https://doi.org/10.2118/190155-ms.

Zhang, F., Saputra, I.W.R., Parsegov, S.G. et al. 2019b. Experimental and Numerical Studies of EOR for the Wolfcamp Formation by Surfactant Enriched Completion Fluids and Multi-Cycle Surfactant Injection. Presented at the SPE Hydraulic Fracturing Technology Conference Woodlands, TX, USA. https://doi.org/10.2118/194325-ms.

Zhang, S. and Zhu, D. 2017. Inversion of Downhole Temperature Measurements in Multistage Fracture Stimulation in Horizontal Wells. Presented at the SPE Annual Technical Conference and Exhibition, San Antonio, Texas, USA. 19. https://doi.org/10.2118/187322-MS.

Zhang, S. and Zhu, D. 2019. Efficient Flow Rate Profiling for Multiphase Flow in Horizontal Wells Using Downhole Temperature Measurement. Presented at the International Petroleum Technology Conference, Beijing, China. 17. https://doi.org/10.2523/IPTC-19138-MS.

Zhu, D., Hill, D., and Zhang, S. 2018. Using Temperature Measurements from Production Logging/Downhole Sensors to Diagnose Multistage Fractured Well Flow Profile. Presented at the SPWLA 59th Annual Logging Symposium, London, UK. 13.

Zou, A. and Schechter, D. 2017. Investigation of the Oil Recovery Mechanism During Laboratory CO2 EOR Experiments with Unconventional Shale Cores through Compositional Simulation. Presented at the Carbon Management Technology Conference, Houston, Texas, USA. https://doi.org/10.7122/486243-ms.